

Neutron Star Kicks in Isolated and Binary Pulsars: Observational Constraints and Implications for Kick Mechanisms

Chen Wang¹, Dong Lai^{2,1}, J. L. Han¹

ABSTRACT

We study observational constraints on neutron star (NS) kicks for isolated pulsars and for neutron stars in binary systems. We are particularly interested in the evidence of kick-spin alignment/misalignment and its dependence on the neutron star initial spin period. For several young pulsars, X-ray observations of compact nebulae showed that pulsar proper motion is aligned with the spin direction as defined by the symmetry axis of the nebula. We also critically examine the measurements of the proper motion and the projected spin axis from a large sample of pulsars with well-calibrated polarization data. We find that among the two dozen pulsars for which reliable measurements are available, there is a significant correlation between the spin axis and the proper motion. For various NS binaries, including double NS systems, binaries with massive main-sequence star companion and binaries with massive white-dwarf companion, we obtain constraints on the kick magnitudes and directions from the observed orbital characteristics of the system. We find that the kick velocity is misaligned with the the NS spin axis in a number of systems, and the NS spin period (when available) in these systems is generally longer than several hundreds milliseconds. These constraints, together with spin-kick alignment observed in many isolated pulsars, suggest that the kick timescale is hundreds of milliseconds to 1 s, so that spin-kick alignment or misalignment can be obtained depending on the initial spin period of the NS. We discuss the implication of our result for various NS kick mechanisms.

Subject headings: stars: kinematics — pulsars: general — stars: neutron — stars: rotation — binaries: close

¹National Astronomical Observatories, Chinese Academy of Sciences, Jia 20 Datun Road, Chaoyang District, Beijing, 100012, China; wangchen@bao.ac.cn, hjl@bao.ac.cn

²Department of Astronomy, Cornell University, Ithaca, NY 14853; dong@astro.cornell.edu

1. Introduction

It has long been recognized that neutron stars (NSs) may have received large kick velocities at birth. First, the measured NS velocities, several hundreds km s^{-1} , are much larger than their progenitors' velocities (e.g., Lorimer et al. 1997; Hansen & Phinney 1997; Arzoumanian et al 2002; Chatterjee et al. 2005; Hobbs et al. 2005; see §2 below). Second, while large space velocities can in principle be accounted for by binary break-up (see Iben & Tutukov 1996), many observed characteristics of NS binaries can be explained only if there is a finite kick at NS birth (e.g., Dewey & Cordes 1987; Yamaoka et al. 1993; Kaspi et al. 1996; Fryer & Kalogera 1997; Fryer et al. 1998; Wex et al. 1999; Stairs et al. 2003; Dewi & van den Heuvel 2004; Willem et al. 2004; Thorsett et al. 2005; see §3). In addition, direct observations of many nearby supernovae (e.g., Wang 2004; Leonard & Filippenko 2004) and supernova remnants (e.g. Hwang et al. 2004) show that supernova explosions are not spherically symmetric, consistent with the existence of NS kicks.

While the evidence for NS kicks is unequivocal, the physical origin remains unclear. The proposed mechanisms include hydrodynamical instabilities in the collapsed supernova core, asymmetric neutrino emission induced by super strong magnetic fields and post-natal electromagnetic boost (see Lai 2004; Janka et al. 2004 and references therein; see §4). One of the reasons that it has been difficult to spin down the kick mechanisms is the lack of correlation between NS velocity and the other properties of NSs. The situation has changed with the recent X-ray observations of the compact X-ray nebulae of several young pulsars, which indicate an approximate alignment between the pulsar proper motion and its spin axis (see Lai et al. 2001; Romani & Ng 2003). For a number of NS binary systems, possible spin-kick relationship can be probed from the observed binary property (e.g. geodetic precession; see §3). It is therefore useful to see whether a consistent picture about NS kicks can be obtained from the two sets of observational constraints.

In this paper we seek empirical constraints on the kick mechanism. We are particularly interested in the possible alignment/misalignment between the kick and the angular momentum of the NS, and how such alignment/misalignment depends on the NS initial spin period. In §2, we summarize and update relevant observational data on isolated pulsars. In addition to several young pulsars for which the spin axis can be measured from the pulsar wind nebula, one can also constrain the spin axis from well-calibrated polarization data. We critically assess the information from such polarization study and demonstrate a correlation between spin axis and proper motion for these pulsars (see Fig. 1). In §3 we discuss constraints on NS kicks in various types of NS binaries. In addition to several well-studied NS/NS binaries, we also consider other types of binaries, such as pulsar/main-sequence and pulsar/white-dwarf binaries. We show that in general, the kick direction is misaligned with the NS spin axis.

We discuss the implications of our findings in §4.

2. Kicks in Isolated Pulsars

By now a number of statistic studies on pulsar velocity have been carried out (e.g., Lyne and Lorimer 1994; Lorimer et al. 1997; Hansen & Phinney 1997; Cordes & Chernoff 1998; Arzoumanian et al 2002; Hobbs et al. 2005). These studies give a mean birth velocity $100 - 500 \text{ km s}^{-1}$, with possibly a significant population having $V \gtrsim 1000 \text{ km s}^{-1}$. Arzoumanian et al. (2002) favor a bimodal pulsar velocity distribution, with peaks around 100 km s^{-1} and 500 km s^{-1} . An analysis of the velocities of 14 pulsars with parallax by Chatterjee et al. (2005) yields a similar result (with $\sigma_v \simeq 100 \text{ km s}^{-1}$ and 300 km s^{-1}). Another recent study of 73 young pulsars by Hobbs et al. (2005) gives a mean 3D pulsar velocity of 400 km s^{-1} , consistent with a single Gaussian distribution.

Despite some early claims, there is currently no statistically significant correlation between the pulsar velocity and the period or the dipole magnetic field strength (as inferred from P, \dot{P}) (e.g., Lorimer et al. 1995). This lack of correlation is not surprising given the large systematic error in the analysis. From a physics point of view, it is also not surprising: (1) The observed spin period for young pulsars is 10 ms or longer, much too slow compared to the breakup rotation rate of a NS (period 1 ms or less); such a slow rotation would not play any dynamically important role in the supernova explosion. (2) The currently observed dipole field of pulsars is 10^{12-14} G , much weaker than the 10^{15-16} G fields required for magnetic field to affect the explosion dynamics or neutrino emission in proto-NSs (see §4).

The lack of correlation between the velocity and the other property of pulsars has been one of the reasons that theoretical models of kicks are not well constrained. However, recent X-ray observation of compact nebulae around several young pulsars has provided evidence for spin-kick alignment; these are summarized in §2.1. Another way of constraining the pulsar spin axis is through radio polarization profile (§2.2).

2.1. Spin-Kick Correlation from Study of Pulsar Wind Nebulae

Recent *Chandra* observations of the pulsar wind nebulae (PWN) have provided evidence for spin-kick alignment for several pulsars (e.g., Pavlov et al. 2000; Helfand et al. 2001; Lai et al. 2001; Ng & Romani 2004; Romani 2004; see Table 1). In particular, the X-ray nebulae of the Crab and Vela pulsars have a two-sided asymmetric jet at a position angle coinciding with the position angle of the pulsar’s proper motion (Pavlov et al. 2000; Helfand et al. 2001).

The symmetric morphology of the nebula with respect to the jet direction strongly suggests that the jet is along the pulsar’s spin axis. Analysis of the polarization angle of Vela’s radio emission corroborates this interpretation (Lai et al. 2001; Radhakrishnan & Deshpande 2001). Ng & Romani (2004) performed a systematic image analysis of pulsar wind tori to determine the pulsar spin axis, and found that several other cases for spin-kick alignment.

In Table 1 we list all the pulsars with the projected rotation axis position angle Ψ_{rot} as determined from PWN symmetry axis, the proper motion position angle Ψ_{PM} , and their difference $|\Delta\Psi_{\Omega\cdot v}|$. In addition, we list the polarization angle Ψ_{pol} where available (see §2.2) and its difference from the proper motion position angle $|\Delta\Psi_{\text{pol}\cdot v}|$. For each pulsar, we obtain the initial spin period P_i using the standard equation

$$P_{\text{init}} = P_0 \left(1 - \frac{n-1}{2} \frac{\tau}{\tau_c} \right)^{1/(n-1)}, \quad (1)$$

where P_0 is the observed period, τ_c is the characteristic age, n is the breaking index, and τ is the true age of the system. We summarize the key results in the following (see Table 1).

Table 1: Spin and proper motion directions for young pulsars with the spin axis determined from PWN

PSR	Ψ_{rot} deg	Ψ_{PM} deg	$ \Delta\Psi_{\Omega\cdot v} $ deg	Ψ_{pol} deg	$ \Delta\Psi_{\text{pol}\cdot v} $ deg	τ kyr	τ_c kyr	P_0 ms	P_{init} ms
B0531+21	124.0 ± 0.1	292 ± 10	12 ± 10	-60 ± 10	8 ± 20	0.95	1.24	33.1	19
J0538+2817	155 ± 8	328 ± 4	7 ± 9			30 ± 4	618	143.2	139.7 ± 0.5
B0833-45	130.6 ± 0.1	301 ± 2	8.6 ± 4	35 ± 10	86 ± 12	...	11.4	89.3	$\lesssim 70$
B1706-44	163.6 ± 0.7	160 ± 10	3.6 ± 11	72 ± 10	88 ± 20	8.9	17	102.5	76 ± 4
B1951+32	85 ± 5	252 ± 7	13 ± 9			64 ± 18	107	39.5	27 ± 6
J1124-5916				22 ± 7		2.5	2.9	135.3	65 ± 20

PSR B0531+21 (Crab pulsar). The breaking index of the Crab pulsar has been measured to be 2.51 ± 0.01 between glitches (Lyne et al. 1993). Eq. (1) thus gives $P_{\text{init}} = 19$ ms. Caraveo & Mignani (1999) report a *HST*-derived proper motion for the Crab pulsar, $(\mu_\alpha, \mu_\delta) = (-17 \pm 3, 7 \pm 3)$ mas yr $^{-1}$, or $\mu = 18 \pm 3$ mas yr $^{-1}$ (implying projected space velocity $v_\perp = 140$ km s $^{-1}$) with a position angle $\Psi_{\text{PM}} = 292^\circ \pm 10^\circ$. Ng & Romani (2004) fitted the two Crab tori of the PWN found in the *CXO* images, and gave the spin direction, $\Psi = 124.0^\circ \pm 0.1^\circ$ and $\Delta\Psi_{\Omega\cdot v} = 12^\circ \pm 10^\circ$.

PSR J0538+2817. This 143 ms pulsar (Lewandowski et al. 2004) is associated with the supernova remnant S147. From the measured proper motion (67_{-22}^{+48} mas yr $^{-1}$) and the separation of the pulsar from SNR center (2.2×10^6 mas), Kramer et al. (2003) deduce the true

age of the pulsar and the remnant, $\tau = 30 \pm 4$ kyr, which is a factor of 20 times less than the pulsar's characteristic age, $\tau_c = 618$ kyr. This implies an initial spin period of $P_{\text{init}} = 139$ ms. The PWN morphology indicates the spin axis at a position angle of $\Psi_{\text{rot}} = 155^\circ \pm 8^\circ$ (Ng & Romani, 2004), which differs from the proper motion axis ($328^\circ \pm 4^\circ$) by less than one σ (Romani & Ng 2003).

PSR B0833-45. The Vela pulsar has $P_0 = 89.3$ ms and $\tau_c = 11.4$ kyr, and is associated with the large Vela supernova remnant. The real age of the pulsar is not known precisely. Using $\tau/\tau_c \gtrsim 0.5$, and $n \gtrsim 1.5$, we obtain an upper limit of the initial period, $P_{\text{init}} < 70$ ms. The Vela pulsar *CXO* ACIS images have a typical double tori structure, from which Ng & Romani (2004) deduce the polar axis direction of $\Psi_{\text{rot}} = 130.6^\circ \pm 0.1^\circ$. Dodson et al. (2003) have measured the proper motion and parallax ($\mu_{\alpha \cos \delta} = -49.68 \pm 0.06$ mas yr $^{-1}$, $\mu_\delta = 29.9 \pm 0.1$ mas yr $^{-1}$ and a distance of 287^{+19}_{-17} pc), which give transverse space velocity $V_T = 61 \pm 2$ km s $^{-1}$, and $\Psi_{\text{PM}} = 301^\circ \pm 2^\circ$. This vector lies $8.6 \pm 4^\circ$ from the fitted torus axis.

PSR B1706-44. This $P_0 = 102.5$ ms pulsar has a spindown age of 17.4 kyr (Wang et al. 2000). It is supposed on the outer edge of a shell-type supernova remnant G343.1-2.3, implying a likely association and the pulsar proper motion direction $\Psi_{\text{PM}} = 160^\circ \pm 10^\circ$ (e.g. McAdam et al. 1993; Dodson & Golap 2002; Bock & Gvaramadze 2002). A best fit of a thermal spectrum to the X-ray emission from the SNR gives a distance of 3.1 kpc, and an age of 8.9 kyr (Dodson & Golap 2002). From eq. (1) we find $P_{\text{init}} = 78$ ms for $n = 1.5$ and $P_{\text{init}} = 72$ ms for $n = 3$. Romani et al. (2005) fit the tori of PWN and obtain the polar axis direction $\Psi_{\text{rot}} = 163.6^\circ \pm 0.7^\circ$, and $\Delta\Psi_{\Omega \cdot v} = 15^\circ \pm 11^\circ$.

PSR B1951+32. This rapidly spinning ($P_0 = 39.5$ ms) radio, X-ray, and γ -ray pulsar is located on the edge of the unusual SNR CTB80 (Kulkarni et al. 1988; Hobbs et al. 2004). The four epochs between 1989 and 2000 show a clear motion for the pulsar of 25 ± 4 mas yr $^{-1}$ at a position angle $252^\circ \pm 7^\circ$, corresponding to a transverse velocity 240 ± 40 km s $^{-1}$ for a distance to the source of 2 kpc (Migliazzo et al. 2002). The offset between the pulsar and the center of its associated supernova remnant implies an age for the pulsar 64 ± 18 kyr, somewhat less than its characteristic age of 107 kyr, from which they give $P_{\text{init}} = 27 \pm 6$ ms (for $n=1.5 - 3.0$). From the pulsar's polar jets, Ng & Romani (2004) measure the spin axis at $\approx 265^\circ \pm 5^\circ$, which is 13° ($\sim 1.4\sigma$) away from the proper-motion axis.

Finally, Romani (2004) mentioned another pulsar, PSR J1124-5916, where the misalignment angle may be measurable. This pulsar has a period of 135 ms and a characteristic age of 2900 yr (Camilo et al. 2002), and is associated with the Oxygen-rich composite supernova remnant G292.0+1.8 (Hughes et al. 2001; Gaensler & Wallace 2003). The precise age of SNR G292.0+1.8 is unknown; for estimate we use $\tau = 2500$ yr (e. g., Gonzales & Safi-Harb

2003). Eq. (1) then gives $P_{\text{init}} = 65 \pm 20$ ms. Romani (2004) measured the elongation of the central PWN and compared this with the direction to the explosion center, and obtained the misaligned angle of $\Delta\Psi_{\Omega\cdot v} \approx 22^\circ \pm 7^\circ$.

We note that for three of the pulsars discussed above (see Table 1), the spin axis can be measured from the intrinsic polarization profile (see §2.2). This gives a consistent spin-velocity angle as the measurement from PWN, after one takes into account of the possible orthogonal mode emission from pulsars.

2.2. Spin-Kick Correlation from Polarization Study

The polarization angle of linearly polarized emission from pulsars is related to the dipole magnetic field geometry of the emission region of a NS. At the pulse center, the line of sight and the spin axis are in the same plane as the curved magnetic field line. This provides another constraint of the projected spin axis on the plane of the sky. Note that radio emission from pulsars could have linear polarization parallel or orthogonal to magnetic field. If spin-kick aligns well, the difference between intrinsic polarization angle (IPA) and proper motion could be either 0° (for normal mode emission) or 90° (for orthogonal mode emission).

Previous investigations of spin-velocity correlation based on polarization data have given inconsistent results. Tademaru (1977) found some evidence for alignment from the polarization angle and proper motion data of 10 pulsars. Morris et al. (1979) measured IPA at the pulse center of 40 pulsars, and claimed that the polarization direction is either parallel or perpendicular to the proper motion vector. Anderson & Lyne (1983) did not find any relation between proper motion directions and pulsar spin axis for 26 pulsars. Deshpande et al. (1999) checked a sample of 29 pulsars for which they estimated IPA and proper motions, and did not find any significant matching between IPA and proper motion.

With the new measurements of proper motions of 233 pulsars (Hobbs et al. 2005), it is useful to re-examine the spin-velocity correlation from polarization data available. To this end, we select normal pulsars (with characteristic age less than a few $\times 10^7$ yr) for which the uncertainty of position angle of the proper motion is less than 15 degree (see ATNF pulsar catalog, Manchester et al. 2005; Hobbs et al. 2005). We then search the literature for observations of their polarization properties and rotation measures. Note that many polarization profiles were not well-calibrated in the polarization angle, and some observations have serious (10% or more) instrumental effect. In our analysis, we use high frequency ($\gtrsim 1.4$ GHz) data; low frequency polarization observations are excluded because of the large-uncertainties of measured polarization angle from even a small uncertainty of Faraday rotations. The po-

larization profiles we use are mostly from Parkes observations (Qiao et al. 1995; Manchester 1971; Manchester et al. 1980; Wu, et al. 1993; van Ommen et al. 1997; Han et al. 2005, in preparation), for which we know that their polarization angles were well calibrated. We take the polarization angle at the maximum sweeping rate or about the pulse center, and calculate IPA with the observation frequency and the pulsar rotation measures. We discard the pulsars when the errors of the calculated IPA are greater than 20 degree. Finally, we obtain the difference between the direction of proper motion and IPA, and remove any object with uncertainty of the difference greater than 25 degree. After above procedures, 24 pulsars are left (see Table 2).

In Table 2, the second and third columns give directions of proper motion on the sky plane, Ψ_{PM} , and IPA, Ψ_{pol} . The fourth columns gives the difference angle $|\Psi_{\text{PM}} - \Psi_{\text{pol}}|$. The fifth and sixth columns give current period P_0 and characteristic age τ_c .

Figure 1 shows the number distribution of the angular difference $|\Psi_{\text{PM}} - \Psi_{\text{pol}}|$. A significant peak appears near 90° , and another peak near 0° is also visible. Since the polarization direction is either parallel or perpendicular to the spin axis, the data therefore indicate a significant correlation between the spin and velocity. Given the result of PWN studies (§2.1), the most likely cause for the two peaks is that spin and kick are aligned in many cases, and different pulsars prefer to emit in one of the two orthogonal modes. Obviously, in this interpretation, intrinsic polarization emission favors perpendicular-mode emission for most pulsars.

We note that for older pulsars in the sample, the proper motion may not directly reflect the initial kick direction because of the pulsar motion in the Galactic potential (e.g., Sun & Han 2004). Indeed, three of five old pulsars in Table 2 with $\tau_c \gtrsim 10$ Myr (although the real age τ may be less than τ_c) show appreciable misalignment, possibly because their proper motion directions have been modified by the Galactic potential.

While our paper was in the final phase of preparation, we became aware of the work by Johnston et al. (2005b) which showed a similar spin-velocity correlation as discussed above.

3. Kicks in Binary Neutron Stars

We now study the constraint on NS kicks (both magnitude and direction) from binary pulsar systems, including NS/NS binaries, NS/Main-Sequence Star (MS) binaries, NS/Massive white dwarf (MWD) binaries and high-mass X-ray binaries (HMXBs). A number of previous studies have focused on individual systems, particularly NS/NS binaries (e.g., Wex et al. 2000; Willems et al. 2004; Thorsett et al. 2005 and references therein) and

Table 2: Spin and proper motion directions for 24 pulsars with the spin axis determined from polarization profiles

PSR	Ψ_{PM} deg	Ψ_{pol} deg	$ \Psi_{\text{PM}} - \Psi_{\text{pol}} $ deg	P_0 ms	τ_c yr	References
B0149-16	173.4 ± 3.0	91.5 ± 9.0	81.9 ± 12.0	832.7	$1.02\text{e+}07$	1, 2
B0531+21 [†]	292.0 ± 10.0	120.0 ± 10.0	8.0 ± 20.0	33.1	$1.24\text{e+}03$	3
B0628-28	294.2 ± 2.6	31.4 ± 3.8	82.8 ± 6.4	1244.4	$2.77\text{e+}06$	3, 2
B0736-40	312.9 ± 6.8	161.6 ± 5.3	28.7 ± 12.1	374.9	$3.68\text{e+}06$	4, 3, 2
B0740-28	277.9 ± 4.4	100.8 ± 3.8	2.9 ± 8.2	166.8	$1.57\text{e+}05$	4, 2
B0818-13	169.2 ± 11.9	51.6 ± 4.6	62.4 ± 16.5	1238.1	$9.32\text{e+}06$	1, 2
B0823+26	145.9 ± 1.9	72.5 ± 5.2	73.4 ± 7.1	530.7	$4.92\text{e+}06$	5
B0833-45	301.0 ± 2.0	35.0 ± 10.0	86.0 ± 12.0	89.3	$1.13\text{e+}04$	3
B0835-41	187.3 ± 7.0	97.3 ± 4.3	90.0 ± 11.3	751.6	$3.36\text{e+}06$	4, 2
B0919+06	12.0 ± 0.1	137.2 ± 16.4	54.8 ± 16.5	430.6	$4.97\text{e+}05$	2
B0950+08 [†]	355.9 ± 0.2	82.2 ± 3.8	86.3 ± 4.0	253.1	$1.75\text{e+}07$	4, 2
B1133+16	348.6 ± 0.1	94.7 ± 4.0	73.9 ± 4.1	1187.9	$5.04\text{e+}06$	4, 2
B1237+25	295.0 ± 0.1	138.1 ± 4.4	23.1 ± 4.5	1382.4	$2.28\text{e+}07$	5
B1325-43	3.2 ± 10.4	66.9 ± 11.4	63.7 ± 21.8	532.7	$2.80\text{e+}06$	6
B1426-66	235.9 ± 8.1	51.6 ± 5.9	4.3 ± 14.0	785.4	$4.49\text{e+}06$	4, 2
B1449-64	216.9 ± 2.8	131.3 ± 5.9	85.6 ± 8.7	179.5	$1.04\text{e+}06$	4, 2
B1451-68	252.7 ± 0.6	146.9 ± 3.6	74.2 ± 4.2	263.4	$4.25\text{e+}07$	4, 2
B1508+55	225.7 ± 1.1	28.5 ± 6.3	17.2 ± 7.4	739.7	$2.34\text{e+}06$	5
B1600-49	268.1 ± 6.5	153.9 ± 17.7	65.8 ± 24.2	327.4	$5.09\text{e+}06$	6
B1642-03	353.0 ± 3.2	74.7 ± 6.7	81.7 ± 9.9	387.7	$3.45\text{e+}06$	2
B1706-44	160.0 ± 10.0	72.0 ± 10.0	88.0 ± 20.0	102.5	$1.75\text{e+}04$	3
B1857-26	202.8 ± 0.7	161.6 ± 3.8	41.2 ± 4.5	612.2	$4.74\text{e+}07$	3, 2, 4
B1929+10	65.2 ± 0.2	51.4 ± 16.2	13.8 ± 16.4	226.5	$3.10\text{e+}06$	5
B2045-16	92.4 ± 2.6	178.5 ± 3.8	86.1 ± 6.4	1961.6	$2.84\text{e+}06$	4, 2

[†]Cases where the Ψ_{pol} have an ambiguity due to orthogonal flips.

Note. — REFERENCES: (1) Qiao et al. (1995); (2) van Ommeren et al. (1997); (3) Han et al. (2005); (4) Manchester et al. (1980); (5) Manchester (1971); (6) Wu et al. (1993).

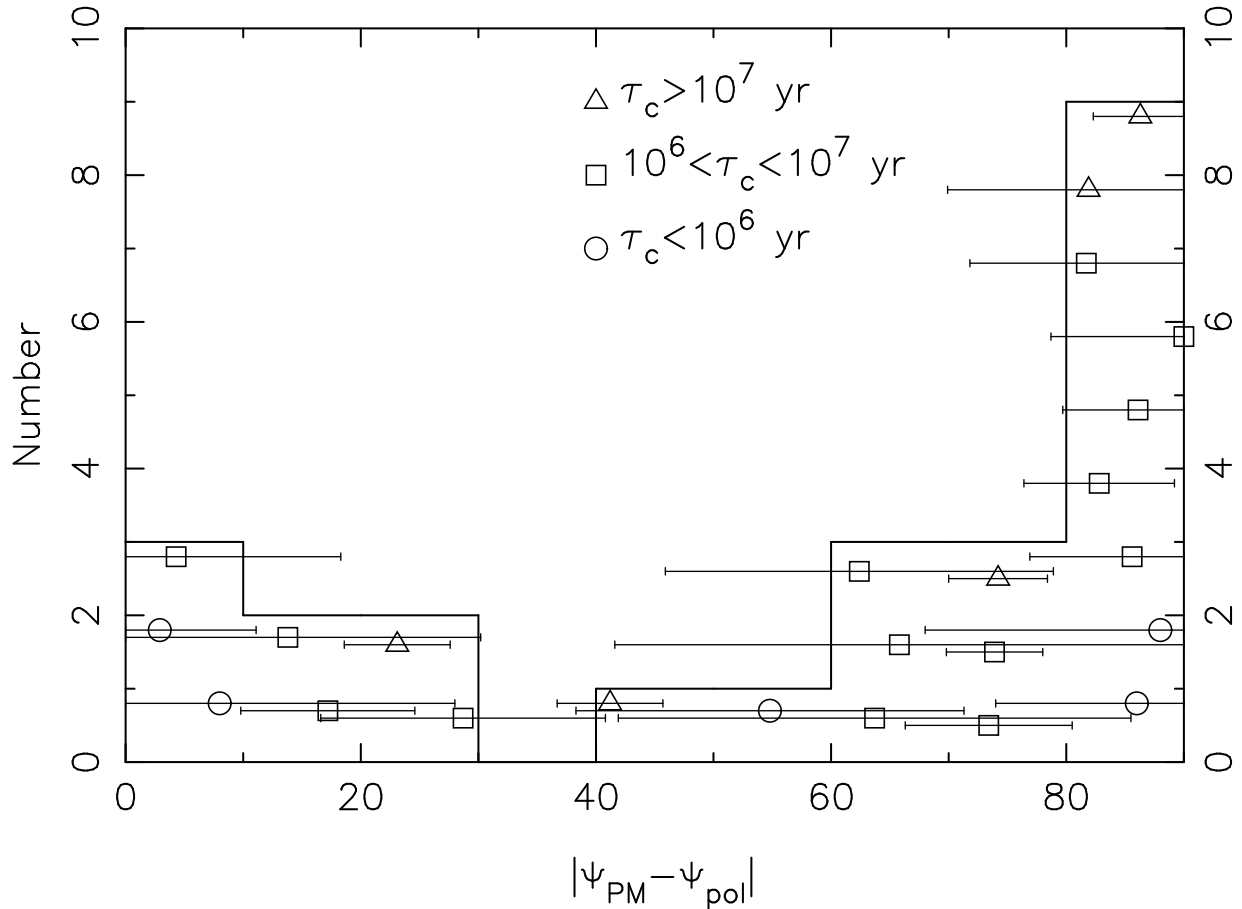


Fig. 1.— The number distribution of the angular difference between the proper motion and intrinsic polarization direction for 24 pulsars. Each pulsar is represented by a symbol specified by the characteristic age of the pulsar.

HMXBs (e.g. Pfahl et al. 2002). Here we consider all systems where such kick constraints are possible.

3.1. Method and Assumptions

The basic procedure for obtaining the constraint is as follows: In the pre-supernova (SN) binary system, we have two stars with mass ¹ m_{Ai} and m_{Bi} in a circular orbit (eccentricity $e_i = 0$) with semi-major axis a_i . Star B is a helium star ready to explode, and its mass $m_{Bi} = m_{He}$ is constrained within the range $2.1 - 8.0 M_{\odot}$ (the lower limit corresponds to the lowest mass for which a He star is expected to form a NS instead of a white dwarf, while the upper limit corresponds to the highest mass for which a He star is expected to form a NS rather than a black hole; see, e.g., Fig.1 in Belczynski et al. 2002, and Table 16.4 in Tauris & van den Heuvel 2004). Star A is either a NS, a massive MS or a massive WD. In the first case, dynamical stability in the mass transfer from the He star to its NS companion requires $m_{Bi}/m_{Ai} \lesssim 3.5$ (see Ivanova et al. 2003). As B explodes in a SN (the explosion can be considered instantaneous compared to the orbital period), it leaves behind a NS with mass $m_B < m_{Bi}$, and because of the asymmetry in the explosion or in the neutrino emission, the NS (in its rest frame) receives a kick velocity \mathbf{V}_k . The angle between \mathbf{V}_k and the pre-SN angular momentum \mathbf{L}_i is γ . To a good approximation, star A is assumed to be unaffected by the explosion of B (see below), i.e., its mass $m_A = m_{Ai}$ after the SN, its post-SN velocity equals the pre-SN velocity. Because of the mass loss and kick in the explosion, the post-SN orbit (with semi-major axis a_f) will in general be eccentric ($e_f \neq 0$), and the orbital angular momentum \mathbf{L}_f will be misaligned relative to \mathbf{L}_i by an angle θ . Using angular momentum conservation and energy conservation, we find

$$V_k^2 = \frac{GM_f}{a_f} [2\xi - 1 + \xi\eta^{-1} - 2(1 - e_f^2)^{1/2}\xi^{3/2}\eta^{-1/2}\cos\theta], \quad (2)$$

$$\cos^2\gamma = \frac{\xi^2(1 - e_f^2)\sin^2\theta}{2\xi - 1 + \xi\eta^{-1} - 2(1 - e_f^2)^{1/2}\xi^{3/2}\eta^{-1/2}\cos\theta}, \quad (3)$$

where $M_f = m_A + m_B$, $M_i = m_A + m_{Bi}$, $\eta = M_f/M_i$ (with $\eta < 1$), and $\xi = a_f/a_i$, which satisfies $(1 + e_f)^{-1} < \xi < (1 - e_f)^{-1}$.

The assumptions leading to eqs. (2)-(3) are fairly standard, and similar equations have been used in numerous previous studies (e.g., Hills 1983). To obtain useful constraint on the kick-spin correlation, we need to make further assumptions about the rotations of the two stars:

¹The subscript “i” specifies parameters before SN, “f” after SN, and “0” currently observed parameters.

Assumption (1): In the pre-SN binary, the assumption of circular orbit made above is justified from the strong tidal interaction and/or mass transfer, which also guarantee that spin angular momentum vectors of the two stars are aligned with the orbital angular momentum vector (i.e., $\mathbf{S}_{\mathbf{A}i} \parallel \mathbf{S}_{\mathbf{B}i} \parallel \mathbf{L}_i$).

As an example, consider the progenitor system of a NS/NS binary: The NS spin $\mathbf{S}_{\mathbf{A}i}$ is expected to be aligned with \mathbf{L}_i because of the mass accretion which spins up the NS. Since the He star is fully convective, the tidal effect on the He star can be estimated using the standard tidal friction theory. Following Zahn (1989; eq. [21]), the tidal circularization time is given by

$$\frac{1}{t_{\text{circ}}} = 21 \frac{\lambda_{\text{circ}}}{t_f} q (1 + q) \left(\frac{R_{\text{He}}}{a_i} \right)^8, \quad (4)$$

where $q = m_{\text{A}}/m_{\text{He}}$ is the mass radio, $t_f = (m_{\text{He}} R_{\text{He}}^2 / L_{\text{He}})^{1/3}$ is the convective friction time ($m_{\text{He}}, L_{\text{He}}$ are the radius and convective luminosity of the He star), and λ_{circ} is a dimensionless average of the turbulent viscosity weighted by the square of the tidal shear. In the prescription of Zahn (1989), λ_{circ} can be approximated by $\lambda_{\text{circ}} \simeq 0.019\alpha^{4/3}(1 + \eta^2/320)^{-1/2}$, where α ($\simeq 2$) is the mixing length parameter and $\eta = 2t_f/P_{\text{orb}}$ measures the timescale mismatch. For the He star parameters, we use the result of Dewi et al. (2002, 2003), who studied the late stage evolution of different types of He-star/NS binaries: (i) Case BA (mass transfer during He core burning) with $m_{\text{He}} = 1.5 - 2.9 M_{\odot}$: the remnants are heavy, degenerate CO white dwarfs (WDs). (ii) Case BB (mass transfer during He shell burning): $m_{\text{He}} = 1.5 - 2.1 M_{\odot}$ produces CO or ONe WDs, $m_{\text{He}} = 2.4 - 2.5 M_{\odot}$ produces ONe WDs and more massive He stars produce NSs. (iii) Case BC (the He star fills its Roche lobe during carbon core burning or beyond) with $m_{\text{He}} = 2.8 - 6.4 M_{\odot}$ producing NSs. Table 3 lists some typical values of m_{He} , R_{He} , L_{He} and P_{orb} for He-star/NS binaries considered by Dewi et al. (2002, 2003), together with the tidal friction time and circularization time as calculated from eq. (4). We see that the tidal circularization time is about one hundred years, and the corresponding synchronization/alignment timescale for the spin of the He star is even shorter [by a factor $\sim (R_{\text{He}}/a_i)^2$]. These timescales are much less than the typical time of mass transfer from the He star prior to its supernova explosion. Thus, the assumption $\mathbf{S}_{\mathbf{A}i} \parallel \mathbf{S}_{\mathbf{B}i} \parallel \mathbf{L}_i$ is very reasonable². We note that the synchronized He star has a large specific angular momentum compared to a maximal-rotating NS. So the He-star core has to shed

²Our analyses here are based on the model of Dewi et al. (2002, 2003), which posits that the He star fills its Roche lobe at certain stage of its evolution. Such Roche-lobe-filling configuration is most likely required for many systems considered here (e.g., PSR J0737-3039 and PSR B1534+12). We note that population studies of binary compact object formation (e.g., Portegies Zwart & Verbunt 1996; Belczynski, Kalogera & Bulik 2002) indicate that a small fraction of progenitors might not be circularized before the explosion.

significant angular momentum before it can collapse to a NS. Such angular momentum loss (most likely mediated by magnetic stress; see Heger et al. 2004) does not change the spin orientation of the He core.

We shall make similar reasonable assumption (that the pre-SN binaries are circular) about MS/He-star binaries (the progenitor systems of MS/NS binaries) and WD/He-star binaries (the progenitor systems of MWD/NS binaries).

Table 3: Tidal circularization timescale of different types of He-star/NS binaries

Case	M_{He} M_{\odot}	R_{He} R_{\odot}	$\text{Log}(L_{\text{He}}/L_{\odot})$	P_{orb} days	t_f yr	t_{circ} yr
BB	2.8	0.5	4.5	0.08	0.01	170
BB	2.8	1.8	4.5	0.5	0.03	100
BB	2.8	2.8	4.5	1.0	0.04	120
BC	2.8	12	4.5	10	0.10	330
BC	3.6	2	5	0.6	0.02	140

Assumption (2): In deriving eqs. (2) and (3), we have assumed that the SN of star B (He star) does not affect the mass and motion of star A. As discussed below, in several systems, the post-explosion spin orientation of star A, \mathbf{S}_{Af} , can be constrained observationally, and we will assume that the spin direction of star A is unchanged during the explosion, i.e. $\mathbf{S}_{\text{Af}} \parallel \mathbf{S}_{\text{Ai}}$.

To justify these assumptions, consider the explosion of the He star in a MS/He-star binary (the progenitor of a MS/NS system)³ and we can estimate the ejecta mass and momentum captured by the MS star. Assuming that the explosion of the He star is only mildly aspherical (indeed, only small asymmetry is enough to generate large kick to the NS), the ejecta mass captured by the MS star is

$$m_{\text{cap}} \sim \frac{\pi R_{\text{MS}}^2}{4\pi a_i^2} m_{\text{ej}} \quad (5)$$

where R_{MS} is the radius of the MS star, a_i the binary separation before explosion, and m_{ej} is the total mass ejected by the He star. As an estimate, we use the parameters for the PSR J0045-7319/MS system (see §3.3 below): From the observed semi-major axis a_0 and eccentricity e_0 of the current PSR/MS binary, we find $a_i > a_f(1 - e_f) \simeq a_0(1 - e_0) \simeq 4R_{\text{MS}}$. Thus at most 1/64 of the ejecta mass is captured by the MS star, or $m_{\text{cap}} \lesssim 0.03M_{\odot}$ for $m_{\text{ej}} =$

³The effect of ejecta capture by the NS in a NS/He-star binary is obviously much smaller.

$m_{\text{He}} - m_{\text{NS}} \sim 2M_{\odot}$. For a typical mass ejection velocity $V_{\text{ej}} \sim 10^4 \text{ km s}^{-1}$, the MS star will receive an impact velocity ΔV less than 30 km s^{-1} . In general, requiring $\Delta V = m_{\text{cap}} V_{\text{ej}} / m_{\text{MS}}$ to be less than pre-explosion orbital velocity of the MS star, $(Gm_{\text{tot}}/a_i)^{1/2} m_{\text{He}} / m_{\text{tot}}$ (where $m_{\text{tot}} = m_{\text{MS}} + m_{\text{He}}$), leads to the condition $a_i \gtrsim 2R_{\text{MS}}$. Thus the momentum impact on the MS star due to the ejecta is negligible in most cases. We note that even in extreme cases, when $a_i/R_{\text{MS}} = \text{a few}$, the momentum impact is along the pre-SN orbital plane. This impact, by itself, does not change the orientation of the orbital plane.

From the above considerations, we conclude that the assumption $\mathbf{S}_{\mathbf{Ai}} \parallel \mathbf{S}_{\mathbf{Bi}} \parallel \mathbf{L}_i \parallel \mathbf{S}_{\mathbf{Af}}$ is most likely valid. Thus the angle θ between \mathbf{L}_i and \mathbf{L}_f is equal to the angle between \mathbf{L}_f and $\mathbf{S}_{\mathbf{Af}}$, which can be constrained observationally (see below).

What about spin orientation $\mathbf{S}_{\mathbf{Bf}}$ of the newly formed NS (star B)? Obviously, if the angular momentum of the NS originates entirely from its progenitor, then $\mathbf{S}_{\mathbf{Bf}} \parallel \mathbf{S}_{\mathbf{Bi}}$. But it is possible that even with zero “primordial” rotation, finite NS rotation can be produced by off-centered kicks (Spruit & Phinney 1998; see also Burrows et al. 1995, who reported a proto-NS rotation period of order 1 s generated by stochastic torques in their 2D supernova simulations). Such SN-generated spin will necessarily make $\mathbf{S}_{\mathbf{Bf}}$ misalign with $\mathbf{S}_{\mathbf{Bi}}$. Thus in general, the angle γ in eq. (3) refers to the angle between the kick \mathbf{V}_k imparted on star B and its primordial spin $\mathbf{S}_{\mathbf{Bi}}$, not necessarily the angle between \mathbf{V}_k and $\mathbf{S}_{\mathbf{Bf}}$ (see §4).

Finally, the post-SN binary may continue to evolve, so the currently observed orbital elements a_0 , e_0 may not be the same as a_f , e_f . Depending on the type of systems, the evolution may be driven by gravitational radiation or tidal effect.

3.2. NS/NS Binaries

Currently there are 8 observed NS/NS binary systems observed in our Galaxy (7 are listed in Stairs 2004, plus PSR J1756-2251 reported by Faulkner et al. 2005)⁴ They consist of a recycled millisecond pulsar (A) and a second-born NS (B) which, in most cases, is not visible as a radio pulsar (with the exception of the double pulsar system, PSR J0737-3039).

Following the birth of the second-born NS (B) in a SN, the NS/NS binary evolution is

⁴Our Table 4 does not include the new system PSR J1906+0746 ($P_{\text{orb}} = 3.98 h$, $e = 0.0853$, $M_{\text{tot}} = 2.6 M_{\odot}$) recently discovered by Arecibo (Lorimer et al. 2005). With the reasonable assumptions that $m_{\text{Ai}} = 2.1 - 8.0 M_{\odot}$, $m_A = m_B = 1.3 M_{\odot}$ and $\theta = 0^\circ - 180^\circ$, we can give the kick velocity $V_k = 50 - 1590 \text{ km s}^{-1}$ and the misalignment between kick and pre-spin axis $\gamma = 24^\circ - 156^\circ$.

governed by gravitational radiation reaction, with (Peters 1964)

$$\frac{1}{a} \frac{da}{dt} = -\frac{64G^3}{5c^5} \frac{m_A m_B M_f}{a^4 (1-e^2)^{7/2}} \left(1 + \frac{73}{24} e^2 + \frac{37}{96} e^4 \right), \quad (6)$$

$$\frac{1}{e} \frac{de}{dt} = -\frac{304G^3}{15c^5} \frac{m_A m_B M_f}{a^4 (1-e^2)^{5/2}} \left(1 + \frac{121}{304} e^2 \right). \quad (7)$$

The time lapse T since the SN to the present is unknown. In our calculations below we adopt the characteristic age of the pulsar, $\tau_c = P/(2\dot{P})$, as a conservative upper limit to T , although the actual value of T may be a lot smaller (see below for specific cases). From the measured a_0 and e_0 , we can integrate eqs. (6)-(7) backward in time to obtain a_f and e_f . We also note that the angle between \mathbf{S}_A and \mathbf{L}_f is unchanged during the evolution and is given by θ .

We now consider individual NS/NS binary systems (see Table 4). The kicks in PSR J0737-3039, PSR B1534+12, PSR B1913+16 have been studied in detail by Willems et al. (2004) (see also Dewi & van den Heuvel 2004; Piran & Shaviv 2004) and PSR B1534+12 by Thorsett et al. (2005). Our constraints on the kick are based on the observed orbital elements and spin parameters of the systems. For several of the systems, additional constraint can be obtained from the proper motion and location of the binary in the Galaxy. We summarize our key findings below (see Table 4).

PSR J0737-3039. This double-pulsar system contains 22.7 ms pulsar (Pulsar A) and a 2.77 s pulsar (Pulsar B), with the current orbital period $P_{\text{orb}}=0.1$ d and eccentricity $e_0=0.0878$ (Lyne et al. 2004). For the He progenitor mass of pulsar B, we consider both the range $m_{\text{Bi}} = 2.1 - 4.7 M_\odot$ (for stable mass transfer) as well as the range $m_{\text{Bi}} = 2.3 - 3.3 M_\odot$ as suggested by Dewi & van den Heuvel (2004). The spindown time of pulsar A is 210 Myr and pulsar B 50 Myr; we use the latter as the approximate upper limit for the time lapse since the SN, thus we consider $e_f=0.0878 - 0.103$ and $a_f=2.94 - 3.28$ ls. The angle θ has not be measured directly. Theoretical modeling of the eclipse lightcurve (Lyutikov & Thompson 2005) suggests that pulsar-B's spin axis \mathbf{S}_{Bf} is inclined from the orbital angular momentum vector by 60° (or 120°); if $\mathbf{S}_{\text{Bf}} \parallel \mathbf{S}_{\text{Bi}}$ (see §3.1), then this angle is equal to θ . Our constraints on V_K and γ for different cases are given in Table 4. For the same input parameters ($\theta = 0^\circ - 180^\circ$, $m_{\text{Bi}} = 2.1 - 4.7 M_\odot$), our result is consistent with that of Willems et al. (2004) (see their Table 2). With the more constrained parameters, we obtain stronger constraints on the kick: for $\theta = 60^\circ$, the kick direction is $\gamma = 36^\circ - 47^\circ$ or $133^\circ - 144^\circ$ with velocity $V_k = 610 - 760$ km s $^{-1}$; for $\theta = 120^\circ$, even larger kicks ($V_k = 1040 - 1300$ km s $^{-1}$) are required⁵.

⁵Such large kick velocities are likely inconsistent with the small measured proper motion of the system

Table 4: Constraints on kicks in double NS binaries

PSR	m_B	m_A	m_{Bi}	e_f	a_f	θ	γ	V_k
	M_\odot	M_\odot	M_\odot		ls	deg	deg	km s^{-1}
J0737-3039	1.25	1.34	2.1–4.7	0.088–0.103	2.94–3.28	0–180	24–156	60–1610
	1.25	1.34	2.3–3.3	0.088–0.103	2.94–3.28	0–180	28–152	80–1490
	1.25	1.34	2.3–3.3	0.088–0.103	2.94–3.28	60	36–47 or 133–144	610–760
J1518+4904	1.05	1.56	2.1–8.0	0.249	56.68	0–180	19–161	11–500
	1.31	1.31	2.1–8.0	0.249	56.68	0–180	12–168	4–500
B1534+12	1.35	1.33	2.1–8.0	0.274–0.282	7.63–7.82	21–29	10–74 or 106–170	160–480
	1.35	1.33	2.1–8.0	0.274–0.282	7.63–7.82	151–159	75–83 or 97–105	660–1360
J1756-2251	1.20	1.37	2.1–8.0	0.181–0.197	6.27–6.65	0–180	20–160	31–1390
J1811-1736	1.11	1.62	2.1–8.0	0.828	96.58	0–180	0–180	0–873
	1.37	1.37	2.1–8.0	0.828	96.58	0–180	0–180	0–867
J1829+2456	1.36	1.14	2.1–8.0	0.139–0.149	14.78–15.47	0–180	20–160	19–867
	1.25	1.25	2.1–8.0	0.139–0.149	14.78–15.47	0–180	22–158	25–870
B1913+16	1.39	1.44	2.1–8.0	0.617–0.657	6.51–7.44	12–24	0–84 or 96–180	180–660
	1.39	1.44	2.1–8.0	0.617–0.657	6.51–7.44	156–168	77–87 or 93–103	530–2170
B2127+11C	1.36	1.35	2.1–8.0	0.681–0.725	6.57–7.81	0–180	0–180	0–2370

Additional constraint from the observed proper motion and galactic location of the system tends to rule out the high values of kick velocity (see Piran & Shaviv 2004; Willems et al. 2004), but does not change the fact that a misaligned kick ($\gamma \neq 0$) is required to explain the observed orbital property of the system.

PSR J1518+4904 contains a 40.9 ms pulsar with $P_{\text{orb}} = 8.634$ d and $e_0 = 0.249$ (Nice, Sayer & Taylor 1996; Hobbs et al. 2004). Thorsett & Chakrabarty (1999) gave the total mass $M_f = m_A + m_B = 2.62(7)M_\odot$, and $m_A = 1.56_{-0.44}^{+0.13}$, $m_B = 1.05_{-0.11}^{+0.45}$. The spindown age of this pulsar is 16 Gyr, According to eqs. (6)-(7), we find that the eccentricity and semi-major axis have changed very little, $a_f \simeq a_0$, $e_f \simeq e_0$. The spin-orbit inclination angle θ for Pulsar A is currently unknown (although it will likely be constrained by measuring geodetic precession in the next few years), so we consider the full range $\theta = 0 - 180^\circ$. For $M_{Bi} = 1.05M_\odot$, the kick direction is constrained to $19^\circ - 161^\circ$ and the kick velocity could be as small as 10 km s^{-1} . For more typical masses, $M_A = 1.32 M_\odot$, $M_B = 1.30 M_\odot$, the kick constraints are similar.

PSR B1534+12 contains a 37.9 ms pulsar with $P_{\text{orb}} = 0.42$ d and $e_0 = 0.274$. Measurement of geodetic precession of the pulsar constrains the spin-orbit inclination angle $\theta = 25^\circ \pm 4^\circ$ or $\theta = 155^\circ \pm 4^\circ$ (Stairs et al. 2004; Thorsett et al. 2005). The spindown time is 250 Myr, and according to eqs. (6)-(7), we obtain the range $e_f = 0.274 - 0.282$, $a_f = 7.63 - 7.82$ ls. For $\theta = 25^\circ \pm 4^\circ$, our result ($V_k \simeq 160 - 480 \text{ km s}^{-1}$) is consistent with Thorsett et al. (2005), who used additional constraint from proper motion ($\mu_\alpha = 1.34(1) \text{ mas yr}^{-1}$, $\mu_\delta = -25.05(2) \text{ mas yr}^{-1}$; with the distance of 0.68 kpc, this corresponds to transverse velocity of $V_T = 107.04 \text{ km s}^{-1}$; Konacji et al. 2003) to obtain $V_k = 230 \pm 60 \text{ km/s}$. The $\theta = 155^\circ \pm 4^\circ$ solution leads to much greater values of V_k and might be inconsistent with the observed proper motion. In all cases, aligned kicks ($\gamma = 0$) are ruled out.

PSR J1756-2251 contains 28.5 ms pulsar with $P_{\text{orb}} = 0.32$ d and $e_0 = 0.181$ (Faulkner et al. 2005). The total system mass $m_A + m_B = 2.574 M_\odot$ from measurement of relativistic periastron advance, and the companion mass is constrained to $m_B < 1.25 M_\odot$. We adopt $m_B = 1.2M_\odot$ and $m_A = 1.37M_\odot$, $\theta = 0^\circ - 180^\circ$. The spin down age is 443 Myr. The kick direction is constrained in $20^\circ - 160^\circ$, which means that aligned kicks are ruled out.

PSR J1811-1736 contains a 104.2ms pulsar with $P_{\text{orb}} = 18.8$ d and $e_0 = 0.828$ (see Stairs 2004). The mass ranges are $m_A = 1.62_{-0.55}^{+0.22}$, $m_B = 1.11_{-0.15}^{+0.53}$. The spindown age is about 900 Myr. For $\theta = 0^\circ - 180^\circ$, the kick is not well constrained. Aligned kicks are allowed

($V_T < 30 \text{ km/s}$; see Kramer et al. 2005; Coles et al. 2005) unless the system has significant line-of-sight velocity. One may thus rule out the Lyutikov-Thompson solution ($\theta = 60^\circ$ or 120°), or, more likely, if the the Lyutikov-Thompson solution is correct, one may conclude that \mathbf{S}_{Bf} is not parallel to \mathbf{S}_{Bi} .

for relatively low m_{Bi} .

PSR J1829+2456 contains a 41 ms pulsar ($\tau_c = 12.4$ Gyr) with $P_{\text{orb}} = 1.18$ d and $e_0 = 0.139$ (Champion et al. 2004; Champion et al. 2005). The masses are $m_A = 1.14^{+0.28}_{-0.48}$ and $m_B = 1.36^{+0.50}_{-0.17}$. The kicks are constrained with $\gamma = 20^\circ - 160^\circ$ and $V_k = 20 - 880 \text{ km s}^{-1}$, which means spin-kick misaligned. For $m_A = m_B = 1.25 M_\odot$, the constraints are similar.

PSR B1913+16 (Hulse-Taylor binary) contains a 59 ms pulsar with $P_{\text{orb}} = 0.323$ d and $e_0 = 0.617$. Measurement of geodetic precession of the pulsar constrains the spin-orbit inclination angle $\theta = 18^\circ \pm 6^\circ$ or $\theta = 162^\circ \pm 6^\circ$ (Wex et al. 2000; Weisberg & Taylor 2003). The spindown time of the pulsar is 109 Myr, so we adopt $T < 109 \text{ Myr}$, giving $e_f = 0.617 - 0.657$, $a_f = 6.51 - 7.44 \text{ ls}$. For the pre-SN mass of the He star in the range of $2.1 - 8.0 M_\odot$, we get a similar result compared to Willems et al. (2004) (see their Table 2): if $\theta = 18^\circ \pm 6^\circ$, $\gamma = 0^\circ - 84^\circ$ or $96^\circ - 180^\circ$, $V_k \simeq 180 - 660 \text{ km s}^{-1}$; if $\theta = 162^\circ \pm 6^\circ$, $\gamma = 77^\circ - 87^\circ$ or $93^\circ - 103^\circ$, $V_k \simeq 530 - 2170 \text{ km s}^{-1}$. The transverse velocity $V_T = 88 \text{ km s}^{-1}$ ($\mu_\alpha = -2.56(6) \text{ mas yr}^{-1}$, $\mu_\delta = 0.49(7) \text{ mas yr}^{-1}$, see Weisberg & Taylor 2003; and distance 7.13 kpc, see Taylor & Cordes 1993) suggests that the $\theta = 18^\circ \pm 6^\circ$ solution may be more reasonable.

PSR B2127+11C contains 30.53 ms-pulsar with $P_{\text{orb}} = 0.335$ d, $e_0 = 0.681$ and characteristic age 97.2 Myr (Deich & Kulkarni 1996). According to eqs. (6)-(7), we find $e_f = 0.681 - 0.725$, $a_f = 6.57 - 7.81 \text{ ls}$. The kicks are not well constrained, and aligned kicks are allowed by the data. Note that this system lies in the globular cluster M15, and it may have formed by many-body interactions in the cluster core.

Our general conclusion from NS/NS binaries is that modest kicks which are misaligned with the pre-SN orbital angular momentum are required to produce the spin-orbit characteristics of these systems (see also van den Heuvel 2004).

3.3. Pulsar/MS Binaries

There are three published pulsar/MS binary systems (see Table 5)⁶ Such systems evolve from He-star/MS binaries (which in turn evolves from MS/MS binaries) when the He star explodes in a SN to form a NS. After the explosion, the pulsar/MS binary may further evolve under tidal interaction if the orbit is sufficiently compact. The evidence for such tidal evolution is most clear in the PSR J0045-7319 system.

⁶We do not include the system PSR J1638-4715, a 0.764 s pulsar with a Be star companion, with $P_{\text{orb}} \simeq 1800$ d and $e_0 = 0.808$ (A. Lyne 2005, private communication).

Table 5: Constraints on kicks in pulsar/MS binaries

PSR	m_A M_\odot	m_B M_\odot	m_{Ai} M_\odot	e_f	a_f ls	θ deg	γ deg	V_k km s^{-1}
J0045-7319	1.58	8.8	2.1–8.0	0.808	293.96	115–160	53–85 or 95–127	119–740
J0045-7319	1.58	8.8	2.1–8.0	0.950	128.79	115–160	52–87 or 93–128	52–750
J0045-7319	1.58	11	2.1–8.0	0.808	293.96	115–160	53–85 or 95–127	130–800
B1259-63	1.35	10	2.1–8.0	0.870	531.51	0–180	0–180	13–330
B1259-63	1.35	10	2.1–8.0	0.870	531.51	10–40	0–86 or 94–180	22–110
J1740-3052	1.35	12–20	2.1–8.0	0.579	873.26	30–75	0–64 or 116–180	37–240
J1740-3052	1.35	12–20	2.1–8.0	0.579	873.26	105–150	48–80 or 100–132	89–370

PSR J0045-7319 contains a 0.926 s pulsar (with characteristic age 3 Myr) in an orbit with a B star companion (mass= $10 \pm 1 M_\odot$) with $P_{\text{orb}} = 51$ d and $e_0=0.808$ (Kaspi et al. 1996). Timing observation revealed the effects of classical spin-orbit coupling due to the rapid rotation of the B star, including periastron advance and precession of the orbital plane (Kaspi et al. 1996; see also Lai et al. 1995; Wex 1998). This constrains the angle between \mathbf{L} and \mathbf{S}_B (spin axis of the B star) to be $\theta = 20^\circ - 65^\circ$ or $\theta = 115^\circ - 160^\circ$. Timing data also revealed rapid orbital decay, $P_{\text{orb}}/\dot{P}_{\text{orb}} = -0.5$ Myr, which can be naturally explained by dynamical tidal interaction between the pulsar and the B star near periastron, provided that the B star rotation axis is (approximately) opposite to \mathbf{L} (Lai 1996; Kumar & Quataert 1997). We therefore choose the $\theta = 115^\circ - 160^\circ$ solution. Lai (1997) showed that during the dynamical tidal evolution, $a(1 - e)$ is approximately constant. Since tidal interaction tends to align \mathbf{S}_B and \mathbf{L} and the current system has a highly misaligned geometry, the binary should not have evolved very long. We therefore consider the range $e_f = 0.808 - 0.95$ (most likely e_f is rather close to e_0). We find that with different values of e_f , the implied V_k and γ change only slightly: $V_k \simeq 50 - 750 \text{ km s}^{-1}$, and $\gamma \simeq 52^\circ - 87^\circ$ or $93^\circ - 128^\circ$, which implies spin-kick misalignment.

Another important point for this system is that the initial spin of the pulsar can be constrained. A generic theory of dynamical-tide induced orbital decay combined with the currently measured orbital decay rate, yield an upper limit, 1.4 Myr, to the age of the system since the SN (Lai 1996). Since the characteristic age of the pulsar is 3 Myr, we find that the initial spin period of the pulsar is close to the current value, $P_{\text{init}} \gtrsim 0.5$ s.

PSR B1259-63 contains a 47.8 ms pulsar and a Be star companion (mass $m_B \simeq 10 M_\odot$), with $P_{\text{orb}} = 1236.7$ d and $e_0 = 0.870$ (see Wex et al. 1998; Wang, Johnston & Manchester 2004). Because of the large orbital period and the short characteristic age (0.33 Myr), tidal interaction is probably unimportant, i.e., the evolution of the system since the SN is negligible. We therefore adopt $e_f \simeq e_0$ and $a_f \simeq a_0$. (With different e_f , the constraint on the kick is similar.) Although spin-orbital coupling effects are likely important in this system, no self-consistent timing solution has been obtained so far (see Wang et al. 2004; Johnston et al. 2005a) and hence θ has not been measured. For $\theta = 0^\circ - 180^\circ$, the kick velocity is constrained to $10 - 340 \text{ km s}^{-1}$, and the kick direction is unconstrained. In particular, for $\theta = 23^\circ - 42^\circ$, aligned kicks ($\gamma = 0$) are allowed (see Fig. 1). Melatos et al. (1995) modeled the variation of the dispersion measure and rotation measure near periastron produced by the circumstellar disk of the Be star and suggested that the disk is tilted with respect to the orbital plane by $10^\circ - 40^\circ$. For θ in this range, aligned kicks are also allowed.

PSR J1740-3052 contains a 0.57 s pulsar (with characteristic age 0.35 Myr) and an early Be star companion (mass $> 11 M_\odot$), with $P_{\text{orb}} = 231$ d and $e_0 = 0.579$ (Stairs et al. 2001). The large orbital period and small characteristic age imply that tidal evolution has not changed the binary parameters, thus we use $e_f \simeq e_0$. The spin-orbital inclination angle θ lies in the range $30^\circ - 75^\circ$ (or $105^\circ - 150^\circ$) (see Stairs et al. 2003). We find that aligned kicks ($\gamma = 0$) are allowed for this system for $\theta = 30^\circ - 75^\circ$, but not allowed for $\theta = 105^\circ - 150^\circ$.

3.4. Young pulsars with massive white dwarf companions

Such systems are thought to evolve from binaries in which both stars are initially less massive than the critical mass required to produce a NS (Tauris & Sennels 2000; Stairs 2004). The initially more massive star transfers mass to its companion before becoming a WD. If sufficient matter can be accreted by the initially low mass star, it will exceed the critical mass and produce a NS. Should the system remain bound, an eccentric binary with a young NS and a MWD companion will be produced. Two such systems are known (see Table 6).

PSR J1141-6545 contains a WD (mass = $0.986 M_\odot$) and a young pulsar ($P_0 = 0.4$ s, mass = $1.30 M_\odot$), with current orbital period $P_{\text{orb}} = 0.198$ d and $e_0 = 0.172$ (see Bailes et al. 2003). Measurement of geodetic precession constrains the spin-orbit inclination angle to $\theta = 15^\circ - 30^\circ$ (or $150^\circ - 165^\circ$) (see Hotan et al. 2005). From the pulsar’s spindown age (1.46 Myr), we find that the orbit has evolved very little, thus $e_f \simeq e_0 = 0.172$ and $a_f \simeq a_0 = 4.38$ ls. For all reasonable mass of the NS progenitor, aligned kicks are ruled out (see Table 6).

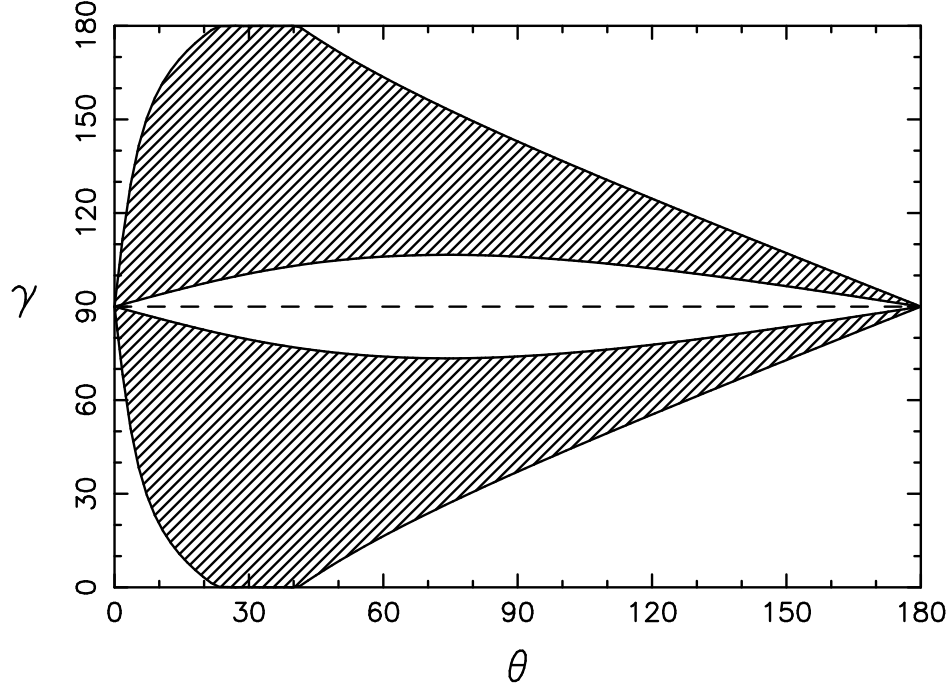


Fig. 2.— The allowed kick angle γ (shaded region) as a function of spin-orbit misalignment angle θ in the PSR B1259-63 system.

Table 6: Constraints on kicks in binary pulsars with massive WD companion

PSR	m_B M_\odot	m_A M_\odot	m_{Bi} M_\odot	e_f	a_f ls	θ deg	γ deg	V_k km s^{-1}
J1141-6545	1.30	0.99	2.1–8.0	0.172	4.38	15–30	21–78 or 102–159	160–620
	1.30	0.99	2.1–8.0	0.172	4.38	150–165	76–85 or 95–104	890–1610
B2303+46	1.34	1.30	2.1–8.0	0.658	72.16	0–180	0–180	0–690

PSR B2303+46 contains a white dwarf (mass= $1.3 M_{\odot}$) and a young pulsar ($P_0=1.1$ s, mass= $1.34 M_{\odot}$), with current orbital period $P_{\text{orb}}=12.34$ d and $e_0=0.658$ (see Thorsett et al. 1993; van Kerkwijk & Kulkarni 1999). The spin-orbital inclination angle θ has not been measured. From the characteristic age of the pulsar (30 Myr), we find that the orbit has evolved very little after the NS’s birth. The kick direction for this system is not constrained.

3.5. High-Mass X-Ray Binaries

A HMXB consists of a NS, which often appears as an X-ray pulsar, and a massive stellar companion (e.g. a Be star). Of the ~ 130 known HMXBs, about 20 have well-constrained orbital elements, mostly determined from the timing of the X-ray pulsars.

Table 7: Constraints on kicks in some Be X-ray binary systems

PSR	P_{orb} days	e_f	m_A M_{\odot}	m_B M_{\odot}	m_{Ai} M_{\odot}	V_k km s^{-1}
4U0115+63	24.32	0.340	1.33	8.00	2.1–8.0	0–470
	24.32	0.340	1.33	20.00	2.1–8.0	3–660
V0332+53	34.25	0.310	1.33	8.00	2.1–8.0	0–410
	34.25	0.310	1.33	20.00	2.1–8.0	0–580
2S1417-624	42.12	0.446	1.33	8.00	2.1–8.0	0–440
	42.12	0.446	1.33	20.00	2.1–8.0	15–620
EXO2030+375	46.01	0.370	1.33	8.00	2.1–8.0	0–360
	46.01	0.370	1.33	20.00	2.1–8.0	5–510
A0535+26	110.3	0.470	1.33	8.00	2.1–8.0	0–320
	110.3	0.470	1.33	20.00	2.1–8.0	13–460

There are three classes of HMXBs, distinguished by their orbital parameters (the first two classes are apparent in Table 3 of Bildsten et al. 1997): (1) Systems with $P_{\text{orb}} \lesssim 10$ days and $e \lesssim 0.1$: The low orbit period and low eccentricity indicate that tidal circularization has played a significant role. So one cannot obtain constraint on NS kicks from the observed orbital parameters. (2) Be X-ray binaries with moderately wide orbits and high eccentricities ($P_{\text{orb}} \sim 20 – 100$ days, $e \sim 0.3 – 0.5$). The high eccentricities indicates these systems have

received large kicks, with a mean speed of $\sim 300 \text{ km s}^{-1}$ (Table 7; see Pfahl et al. 2002). (3) Possibly another class of Be X-ray binaries has recently been identified by Pfahl et al. (2002) (see their Table 1). These systems are distinguished from the well-known Be X-ray binaries by their wide orbits (all have $P_{\text{orb}} > 30$ days) and fairly low eccentricities ($e \lesssim 0.2$). The NSs born in these systems apparently have received only a small kick, $\lesssim 50 \text{ km s}^{-1}$. Pfahl et al. (2002) and van den Heuvel (2004) discussed possible origin for the bimodal kicks in the two classes of Be X-ray binaries.

The eccentric Be X-ray binaries have similar orbital parameters as the pulsar/MS binaries discussed in §3.3. In Table 7 we list 5 Be X-ray binaries which belong to the second class discussed in the previous paragraph. With the reasonable assumptions that the mass of the companion main-sequence star $m_B = 8 - 20 M_{\odot}$, the mass of the NS progenitor $m_{Ai} = 2.1 - 8.0 M_{\odot}$ and the NS mass $m_A = 1.33 M_{\odot}$, the allowed range of kick velocities is given in Table 7. Since the angle θ is unknown, we find the kick directional angle γ is unconstrained for these systems, i.e. $\gamma = 0^\circ - 180^\circ$ (see Table 7), similar to the PSR B1259-63 case (cf. Table 5). The magnitude of the kick velocity ranges from 0 to several hundred km s^{-1} .

4. Discussion

4.1. Tentative Inference from Observational data

Our analysis of the velocity-spin correlation for isolated pulsars (§2) shows that kick is aligned with spin axis for many (but most likely not all) pulsars (see Table 1-2 and Fig. 1). Of particular interest is the fact that for pulsars with estimated initial spin periods (when such estimate can be made) less than ~ 200 ms, the kick is apparently aligned with the spin axis to within the error of measurements (typically $\pm 10^\circ$; see Table 1). If we exclude PSR J0538+281 (for which $P_{\text{init}} \sim 140$ ms), the initial spin periods of these pulsars are all less than ~ 70 ms. Of course, we should add the usual caveat that a pulsar might have experienced a phase of rapid spindown before electromagnetic braking begins, so that the actual spin period of the proto-NS may be shorter than the estimated P_{init} .

On the other hand, our analysis of SN kicks in NS binaries based on the observed spin-orbital property of various NS binaries (§3) shows that in a number of systems, the kick must not be aligned with the spin axis of the *NS progenitor*. How can we reconcile this conclusion with the apparent spin-kick alignment for many isolated pulsars?

One possibility is that although the kick \mathbf{V}_k is misaligned with the spin axis (denoted by \mathbf{S}_{Bi} in §3) of the He star, it may still be aligned with the spin axis of the NS, since the NS

may get most of its angular momentum from off-centered kicks rather than from its He star progenitor (Spruit & Phinney 1998; see also Burrows et al. 1995). However, in the absence of any “primordial” angular momentum from the progenitor, a kick (of any duration) displaced by a distance s from the center, produces a spin of $\simeq 12 (V_k/300 \text{ km s}^{-1})(s/10 \text{ km}) \text{ Hz}$, with the spin axis necessarily perpendicular to the velocity direction. If the kick is the result of many thrusts on the proto-NS (Spruit & Phinney 1998), the relative direction of the net kick and spin depends on how the orientation of each thrust is correlated with each other. Spin-kick alignment is possible in some circumstances, but is by no means a generic prediction of the “multiple thrusts” scenario. If the kick direction is not aligned with the He star spin (as we show for many NS binaries in §3), it will not be aligned with the NS spin in general, regardless of the origin of the NS spin.

An important clue comes from the PSR 0045-7319/B-star system: The kick imparted to the pulsar at its birth is misaligned with its spin axis, and the initial spin period has been constrained to be $P_{\text{init}} > 0.5 \text{ s}$ (see §3.3). Also, for PSR 0737-3039 (with pulsar B spin period $P_0 = 2.77 \text{ s}$) and many other NS/NS binaries, as well as for the PSR J1141-6545/MWD system (with $P_0 = 0.39 \text{ s}$), the kick is misaligned with the spin axis. In addition, for the PSR J1740-3053/MS (with $P_0 = 0.57 \text{ s}$) system, the kick and spin may be misaligned.

Combining these kick constraints obtained from NS binaries with the information we have about kicks in isolated pulsars, we are led to the following tentative suggestion: When the NS initial spin period is less than a few $\times 100 \text{ ms}$, the kick will be aligned with the spin axis; otherwise, the kick will in general not be aligned with the spin axis, except by chance. This suggestion, by no means definitive, is consistent with all the observational data on NS kicks in isolated pulsars and in NS binaries which have been analyzed/summarized in §2 and §3.

We now discuss the implications of this suggestion for NS kick mechanisms.

4.2. Implications for kick mechanisms

Many mechanisms for NS kicks have been suggested or studied. They generally fall into the following categories (e.g., Lai 2004; Janka et al. 2004).

(i) *Hydrodynamically driven kicks* in which the SN explosion is asymmetric (with the explosion stronger in one direction than the other directions), and the NS receives a kick according to momentum conservation. Large-scale convections in the neutrino-heated mantle behind the stalled shock (at $\sim 100 \text{ km}$) may naturally lead to such asymmetric explosion, particularly when the delay between core bounce and shock revival is sufficiently long to

allow for small-scale convective eddies to merge into bigger ones (Scheck et al. 2004; see also Thompson 2000; Blondin & Mezzacappa 2005; Foglizzo et al. 2005). Pre-SN asymmetric perturbations due to convective O-Si burning (Bazan & Arnett 1998), amplified during core collapse (Lai & Goldreich 2000), may also play a role (Burrows & Hayes 1996; Goldreich et al. 1996; Fryer 2004). The kick timescale ranges from 10’s ms to 100’s ms. Obviously, detailed calculations of this class of mechanisms are still uncertain — such a calculation/simulation is an integral part of the general problem of SN explosion mechanism.

(ii) *Magnetic-Neutrino Driven kicks* rely on asymmetric neutrino emission induced by strong magnetic fields. This could arise because the strong magnetic field modifies the neutrino opacities either through standard weak-interaction physics (e.g. Dorofeev et al. 1985; Lai & Qian 1998; Arras & Lai 1999a,b; Duan & Qian 2005) or through nonstandard physics (e.g., Fuller et al. 2003; Lambiase 2005). It could also arise from the dynamical effect of the magnetic field on the proto-NS (e.g., the B field can affect the neutrino-driven convection/instabilities, and thus creating dark or hot neutrino spots; Duncan & Thompson 1992; Socrates et al. 2004). All these effects are important only when the magnetic field of the proto-NS is stronger than 10^{15} G. The kick timescales are of order the neutrino diffusion time, a few seconds.

(iii) *Electromagnetically driven kicks* involve radiation from off-centered rotating dipole, which, for appropriate dipole orientation/displacement, imparts a gradual acceleration to the pulsar along its spin axis (Harrison & Tademaru 1975; Lai et al. 2001). This effect is important only if the NS initial period is $\lesssim 2$ ms. The kick time is of order the initial spin-down time ($\simeq 10^7$ s for $B = 10^{13}$ G and $P_{\text{init}} = 14$ ms).

(iv) Other mechanisms are possible if the collapsing iron core has large angular momentum. For example, the combination of rapid rotation and magnetic field may lead to bipolar jets from the SN, and a slight asymmetry between the two jets will lead to a large kick (e.g. Khokhlov et al. 1999; Akiyama et al. 2003). Another mechanism could be that, if a rapidly rotating core fragments into a double proto-NS binary (current numerical simulation indicates this is unlikely; see Fryer & Warren 2003), the explosion of the lighter proto-NS (after mass transfer) could give the remaining NS a kick (Colpi & Wasserman 2002; see also Davis et al. 2002).

It is of interest to use observations to constrain or rule out some of these mechanisms. Since the initial spin period of radio pulsars is $\gg 1$ ms, (iii) and (iv) appear unlikely in general. The observed dipole magnetic field of most radio pulsars lies in the range $10^{12} - 10^{13}$ G, but it is not clear whether most proto-NSs can have (even transient) magnetic fields stronger than 10^{14} G. So we cannot easily rule out (ii).

Regarding spin-kick alignment/misalignment, the crucial point is the ratio between the initial spin period P_{init} and kick timescale τ_{kick} . In hydrodynamically driven kicks (i) and magnetic-neutrino driven kicks (ii), the primary thrust to the NS does not depend on the NS spin axis. But the net kick will be affected by rotational averaging if P_{init} is much less than τ_{kick} . Let V_0 be the kick velocity that the NS attains in the case of zero rotation, and θ_k be the angle between the primary asymmetry and the rotation axis. The expected components of kick along the rotation axis and perpendicular to it are (for $\tau_{\text{kick}} \gg P_{\text{init}}$)

$$V_{\text{kick}\parallel} = V_0 \cos \theta_k, \quad V_{\text{kick}\perp} \sim \frac{\sqrt{2} P}{2\pi \tau_{\text{kick}}} V_0 \sin \theta_k. \quad (8)$$

Thus the angle γ between the kick vector \mathbf{V}_{kick} and the spin axis is given by $\tan \gamma \sim 0.2(P_{\text{init}}/\tau_{\text{kick}}) \tan \theta_k$. Typically, the spin-kick alignment will be achieved when $\tau_{\text{kick}} \gg P_{\text{init}}$. The observed spin-kick alignment for $P_{\text{init}} \lesssim 100$'s ms discussed in §4.1 therefore suggests that τ_{kick} lies between hundreds of ms to 1 s. Such kick timescale is consistent with magnetic-neutrino driven mechanisms or hydrodynamical mechanisms with long-delayed SN explosions.

Obviously, this conclusion is far from definitive. For example, since the primary thrust may be applied at a distance larger than the NS radius, a somewhat more stringent condition on P_{init} is required to produce spin-kick alignment (see Lai et al. 2001). In another word, the inequality $P_{\text{init}} \ll \tau_{\text{kick}}$ is a necessary (but not sufficient) condition for spin-kick alignment. Also, an initial spin period of order 100's ms could be generated by the SN kick itself (see above). We have argued (see §4.1) that a kick-induced spin without “primordial” angular momentum (i.e. from the progenitor) would not in general give rise to spin-velocity alignment. The situation may be different with even a modest primordial spin. We plan to study these issues in the future.

This work is supported by National Natural Science Foundation of China (10328305, 1025313 and 10473015). DL has also been supported in part by NSF grant AST 0307252 and NASA grant NAG 5-12034. DL thanks IAS (Princeton), CITA (Toronto), Tsinghua University (Beijing) and particularly NAOC (Beijing) for hospitality during the course of the work.

REFERENCES

- Anderson, B. & Lyne, A. G. 1983, Nature, 303, 597
 Akiyama, S., Wheeler, J. C., Meier, D. L., & Lichtenstadt, I. 2003, ApJ, 584, 954

- Arras, P. & Lai, D. 1999a, PhRvD, 60, 3001A
- Arras, P. & Lai, D. 1999b, ApJ, 519, 745
- Arzoumanian, Z., Chernoff, D. F., & Cordes, J. M. 2002, ApJ, 568, 289
- Bailes, M., Ord, S. M., Knight, H. S., & Hotan, A. W. 2003, ApJ, 595, 49
- Bazan, G. & Arnett, D. 1998, ApJ, 496, 316
- Belczynski, K., Kalogera, V., & Bulik, T. 2002, ApJ, 572, 407
- Bildsten, L., Chakrabarty, D., & Chiu, J. et al. 1997, ApJS, 113, 367
- Blondin, J. M. & Mezzacappa, A. 2005, astro-ph/0507181
- Bock, D. C.-J. & Gvaramadze, V. V. 2002, A&A, 394, 533
- Burrows, A. & Hayes, J. 1996, Phys. Rev. Lett., 76, 352
- Burrows, A., Hayes, J., & Fryxell, B. A. 1995, ApJ, 450, 830
- Camilo, F., Manchester, R. N., & Gaensler, B. M. et al. 2002, ApJ, 567, 71
- Caraveo, P. A. & Mignani, R. P. 1999, A&A, 344, 367
- Champion, D. J. et al. 2004, MNRAS, 350, 61
- Champion, D. J. et al. 2005, astro-ph/0508320
- Chatterjee, S., Vlemmings, W. H. T., Cordes, J. M., & Chernoff, D. F. 2005, ApJ, submitted
- Coles, W. A., McLaughlin, M. A., Rickett, B. J., Lyne, A. G., & Bhat, N. D. R. 2005, ApJ, 623, 392
- Colpi, M. & Wasserman, I. 2002, ApJ, 581, 1271
- Cordes, J. M. & Chernoff, D. E. 1998, ApJ, 505, 315
- Davies, M. B., King, A., Rosswog, S., & Wynn, G. 2002, ApJ, 579, 63
- Deich, W. T. S & Kulkarni, S. R. 1996, in Compact Stars in Binaries, ed. J. van Paradijs et al., 279
- Deshpande, A. A., Ramachandran, R., & Radhakrishnan, V. 1999, A&A, 351, 195
- Dewey, R. J. & Cordes, J. M. 1987, ApJ, 321, 780

- Dewi, J. D. M., Podsiadlowski, Ph., & Pols, O. R. 2005, astro-ph/0507628
- Dewi, J. D. M. & Pols, O. R. 2003, MNRAS, 344, 629
- Dewi, J. D. M., et al. 2002, MNRAS, 331, 1027
- Dewi, J. D. M. & van den Heuvel, E. P. J. 2004, MNRAS, 349, 169
- Dodson, R. & Golap, K. 2002, MNRAS, 334, 1
- Dodson, R. G., Legge, D., Reynolds, J. E., & McCulloch, P. M. 2003, ApJ, 596, 1137
- Dorofeev, O. F., Rodionov, V. N., & Ternov, I. M. 1985, SvAL, 11, 123
- Duan, H. Y. & Qian, Y. Z. 2005, astro-ph/0506033
- Duncan, R. C. & Thompson, C. 1992, ApJ, 392, 9
- Faulkner, A. J., Kramer, M. , & Lyne, A. G. et al. 2005, ApJ, 618, 119
- Foglizzo, T., Scheck, L., & Janka, H. -Th. 2005, astro-ph/0507636
- Fryer, Chris L. 2004, ApJ, 601, 175
- Fryer, C., Burrows, A., & Benz, W. 1998, ApJ, 496, 333
- Fryer, C. L. & Kalogera, V. 1997, ApJ, 489, 244
- Fryer, C. L. & Warren, M. S. 2004, ApJ, 601, 391
- Fryer, C. L., Warren, M. S., Holz, D. E., Hughes, S. A., & Dupuis, R. 2003, SPIE, 4856, 123
- Fuller, G. M., Kusenko, A., Mocioiu, I., & Pascoli, S. 2003, PhRvD, 68, 3002
- Gaensler, B. M. & Wallace, B. J. 2003, ApJ, 594, 326
- Goldreich, P., Lai, D., & Sahrling, M. 1996, in "Unsolved Problems in Astrophysics", eds. J.N. Bahcall and J.P. Ostriker (Princeton Univ. Press)
- Gonzalez, M. & Safi-Harb, S. 2003, ApJ, 583, 91
- Han, J. L. et al. 2005, in preparation.
- Hansen, B. M. S. & Phinney, E. S. 1997, MNRAS, 291, 569
- Harrison, E. R. & Tademaru, E. 1975, ApJ, 201, 447

- Heger, A., Woosley, S. E., Langer, N., & Spruit, H. C. 2004, in Stellar Rotation, Proceedings of IAU Symposium No. 215, eds. A. Maeder & P. Eenens, 591
- Helfand, D. J., Gotthelf, E. V., & Halpern, J. P. 2001, *ApJ*, 556, 380
- Hills, J. G. 1983, *ApJ*, 267, 322
- Hobbs, G., Lorimer, D. R., Lyne, A. G., & Kramer, M. 2005, *MNRAS*, 475
- Hobbs, G., Lyne, A. G., & Kramer, M. 2004, *MNRAS*, 353, 1311
- Hotan, A. W., Bailes, M., & Ord, S. M., 2005, *ApJ*, 624, 906
- Hughes, J. P., Slane, P. O., & Burrows, D. N. 2001, *ApJ*, 559, 153
- Hwang, U., Laming, J. M., & Badenes, C. 2004, *ApJ*, 615, 117
- Iben, I. Jr. & Tutukov, A. V. 1996, *ApJ*, 456, 738
- Ivanova, N., Belczynski, K., Kalogera, V., Rasio, F. A., & Taam, R. E. 2003, *ApJ*, 592, 475I
- Janka, H.-T., Scheck, L., & Kifonidis, K. et al. 2004, astro-ph/0408439
- Johnston, S., Ball, L., Wang, N., & Manchester, R. N. 2005a, *MNRAS*, 358, 1069J
- Johnston, S. et al. 2005b, *MNRAS*, submitted
- Kaspi, V. M., Bailes, M., & Manchester, R. N. 1996, *Nature*, 381, 584
- Khokhlov, A. M., et al. 1999, *ApJ*, 524, 107
- Konacki, M., Wolszczan, A., & Stairs, I. H. 2003, *ApJ*, 589, 495
- Kramer, M., Lyne, A. G., & Loehmer, O., et al. 2003, *ApJ*, 593, 31
- Kramer, M., Lorimer, D. R., & Lyne, A. G., et al. 2005, astro-ph/0503386
- Kulkarni, S. R., Clifton, T. C., & Backer, D. C. 1988, *Nature*, 331, 50
- Kumar, P. & Quataert, E. J. 1997, *ApJ*, 479, 51
- Lai, D. 1996, *ApJ*, 466, 35
- Lai, D. 1997, *ApJ*, 490, 847
- Lai, D. 2004, in *Cosmic Explosions in 3D: Asymmetries in Supernovae and Gamma-ray Bursts*. eds. P. Hoflich et al. (Cambridge Univ. Press), p.276 (astro-ph/0312542)

- Lai, D., Bildsten, L., & Victoria M. 1995, ApJ, 452, 819
- Lai, D., Chernoff, D. F., & Cordes, J. M. 2001, ApJ, 549, 1111
- Lai, D. & Goldreich, P. 2000, ApJ, 535, 402L
- Lai, D. & Qian, Y. Z. 1998, ApJ, 505, 844
- Lambiase, G. 2005, MNRAS, 362, 867
- Leonard, D. C. & Filippenko, A. V. 2004, astro-ph/0409518
- Lewandowski, W. et al. 2004, ApJ, 600, 905L
- Lorimer, D. R., Bailes, M., & Harrison, P. A. 1997, MNRAS, 289, 592
- Lorimer, D. R., Lyne, A. G., & Anderson, B. 1995, MNRAS, 275, 16
- Lorimer, D. R. et al. 2005, submitted to ApJ.
- Lyne, A. G., Burgay, M., & Kramer, M. 2004, Science, 303, 1153
- Lyne, A. G. & Lorimer, D. R. 1994, Nature, 369, 127
- Lyne, A. G., Pritchard, R. S., & Smith, F. G. 1993, MNRAS, 265, 1003
- Lyutikov, M. & Thompson, C. 2005, astro-ph/0502333
- Manchester, R. N. 1971, ApJS, 23, 283
- Manchester, R. N., Hamilton, P. A., & McCulloch, P. M. 1980, MNRAS, 192, 153
- Manchester, R. N., Hobbs, G. B., Teoh, A., & Hobbs, M. 2005, AJ, 129, 1993M
- McAdam, W. B., Osborne, J. L., & Parkinson, M. L. 1993, Nature, 361, 516
- Melatos, A., Johnston, S., & Melrose, D. B. 1995, MNRAS, 275, 381
- Migliazzo, J. M., Gaensler, B. M., & Backer, D. C. 2002, ApJ, 567, 141
- Morris, D., et al. 1979, A&A, 73, 46
- Ng, C.-Y. & Romani, R. W. 2004, ApJ, 601, 479
- Nice, D. J., Sayer, R. W., & Taylor, J. H. 1996, ApJ, 466, 87
- Pavlov, G. G., Sanwal, D., & Garmire, G. P. 2000, A&AS, 196, 3704

- Peters, P. C. 1964, Phys. Rev., 136, 1224
- Pfahl, E., Rappaport, S., Podsiadlowski, P., & Spruit H. 2002, ApJ, 574, 364
- Piran, Tsvi & Shaviv, Nir J. 2004, astro-ph/0409651
- Portegies Zwart, S. F. & Verbunt, F. 1996, å, 309, 179P
- Qiao, G., Manchester, R. N., Lyne, A. G., & Gould, D. M. 1995, MNRAS, 274, 572bv
- Radhakrishnan, V. & Deshpande, A. A. 2001, A&A, 379, 551
- Romani, R. W. 2004, astro-ph/0404100
- Romani, R. W. & Ng, C.-Y. 2003, ApJ, 585, 41
- Romani, R. W., Ng, C. -Y., Dodson, R., & Brisken, W. 2005, astro-ph/0506089
- Scheck, L., Plewa, T., Janka, H.-Th., Kifonidis, K., & Mller, E. 2004, PhRvL, 92, 1103S
- Socrates, A., Blaes, O., Hungerford, A., & Fryer, C. L. 2004, astro-ph/0412144
- Spruit, H. C. & Phinney, E. S. 1998, Nature, 393, 139
- Stairs, I. H. 2004, Science, 304, 547
- Stairs, I. H., Manchester, R. N., & Lyne, A. G. et al. 2001, MNRAS, 325, 979
- Stairs, I. H., Manchester, R. N., & Lyne, A. G. et al. 2003, in Radio Pulsars, ASP Conf. Proceedings, ed. M. Bailes, D. J. Nice, & S. E. Thorsett, 302
- Stairs, I. H., Thorsett, S. E., & Arzoumanian, Z. 2004, PhRvL, 93, 1101
- Sun, X. H. & Han, J. L. 2004, MNRAS, 350, 232
- Tademaru, E. 1977, ApJ, 214, 885
- Tauris, T. M. & Sennels, T. 2000, A&A, 335, 236
- Tauris, T. M. & van den Heuvel, E.P.J. 2004, in “Compact Stellar X-Ray Sources”, eds. W.H.G. Lewin and M. van der Klis (Cambridge University Press)
- Taylor, J. H. & Cordes, J. M. 1993, ApJ, 411, 674
- Thompson, C. 2000, ApJ, 534, 915
- Thorsett, S. E., Arzoumanian, Z., McKinnon, M. M., & Taylor, J. H. 1993, ApJ, 405, 29

- Thorsett, S. E., Dewey, R. J., & Stairs, I. H. 2005, ApJ, 619, 1036
- van den Heuvel, E. P. J. 2004, in Proc. of 5th Integral Science Workshop (astro-ph/0407451)
- van Kerkwijk, M. H. & Kulkarni, S. R. 1999, ApJ, 516, 25
- van Ommen, T. D., et al. 1997, MNRAS, 287, 307V
- Wang, N., Johnston, S., & Manchester, R.N. 2004, MNRAS, 351, 599
- Weisberg, J. M. & Taylor, J. H. 2003, ASPC, 302, 93
- Wex, N. 1998, MNRAS, 298, 67
- Wex, N., Johnston, S., & Manchester, R. N. 1998, MNRAS, 298, 997
- Wex, N., Kalogera, V., & Kramer, M. 2000, ApJ, 528, 401
- Wex, N. & Kopeikin, S. M. 1999, ApJ, 514, 388
- Willems, B., Kalogera, V., & Henninger, M. 2004, ApJ, 616, 414
- Wu, Xinji, Manchester, R. N., Lyne, A. G., Qiao, G. 1993, MNRAS, 261, 630W
- Yamaoka, H., Shigeyama, T., & Nomoto, K. 1993, A&A, 267, 433
- Zahn, J.-P. 1989, A&A, 220, 112